Journal of Electromagnetic Waves and Applications

ISSN: 0920-5071 (Print) 1569-3937 (Online) Journal homepage: http://www.tandfonline.com/loi/tewa20

AN IMPROVED NONLINEAR CURRENT MODEL FOR GAN HEMT HIGH POWER AMPLIFIER WITH LARGE GATE PERIPHERY

L. Sang & J. E. Schutt-Aine

To cite this article: L. Sang & J. E. Schutt-Aine (2012) AN IMPROVED NONLINEAR CURRENT MODEL FOR GAN HEMT HIGH POWER AMPLIFIER WITH LARGE GATE PERIPHERY, Journal of Electromagnetic Waves and Applications, 26:2-3, 284-293, DOI: 10.1163/156939312800030820

To link to this article: https://doi.org/10.1163/156939312800030820

J. of Electromagn. Waves and Appl., Vol. 26, 284–293, 2012

AN IMPROVED NONLINEAR CURRENT MODEL FOR GAN HEMT HIGH POWER AMPLIFIER WITH LARGE GATE PERIPHERY

L. Sang[1, 2, *] and J. E. Schutt-Aine[2]

[1]Fundamental Science on EHF Laboratory, University of Electronic Science and Technology of China, China

[2]Department of Electrical and Computer Engineering, University of Illinois at Urbana-Champaign, Urbana, IL 61801, United States

Abstract—According to the characteristics of high power GaN amplifier, the common current-voltage (I-V) temperature dependence model established by Angelov is improved in this research. Besides embodying the surface temperature distribution, the most important improvement is that it can describe the current decreasing trend under high bias voltage due to trapping related dispersion and self-heating effect. The practical application shows that the prediction accuracy of the large signal equivalent circuit model is improved obviously after introducing the proposed I-V model.

1. INTRODUCTION

The design of power amplifier represents a fundamental topic for the microwave community, as clearly demonstrated by an increasing number of papers and books dedicated to this issue published in recent years [1]. The advent of GaN technology has provided new stimuli in this design field foreseeing unbelievable performance in terms of power density, output, gain and power add efficiency (PAE) [2]. Accurate large signal model is crucial for the GaN power device and circuit design. Compared with physical based model and table based empirical model, empirical large signal equivalent circuit model (LSECM) is simpler and easier to be implemented in microwave commercial simulation software, and has been widely used in GaAs and SiC based devices [3, 4]. However, accurate LSECM for GaN based devices is still a major topic of discussion due to the existence of self-heating effect,

---

Received 5 November 2011, Accepted 6 January 2012, Scheduled 13 January 2012

* Corresponding author: Lei Sang (leisang@illinois.edu).

trapping related dispersion and temperature distribution effect in GaN HEMT devices especially high power amplifiers (output more than 40 dBm). The common LSECM is suitable for small gate periphery amplifiers with low output level. Since the GaN high power amplifier which contains more amplifier cells has a lot of special characteristics of current, the common LSECM cannot achieve very accurate simulated performance. In the large signal equivalent circuit model, the I-V model is the most important factor which is the main difference between the two output level devices. In this research, the most common I-V model established by Angelov is improved according to the characteristics of the high power GaN amplifier. The improved I-V model can not only embody the surface temperature distribution by using temperature dependence equations but also describe self-heating effect and trapping related dispersion. The practical validation shows that the predicted result based on the improved I-V model can fit the measured data well, and the accuracy of the simulated output performance of the power amplifier can be improved compared with the original model.

The paper is organized as bellow: the characteristics of high power GaN amplifier with large gate periphery is analyzed in Section 2. The improved I-V model is described in Section 3. In Section 4, a high power GaN amplifier is used to validate the accuracy and practicability. The conclusion is given in Section 5.

2. THE CHARACTERISTIC ANALYSIS OF THE HIGH POWER GAN AMPLIFIER

Fig. 1 shows the measured results of two GaN amplifiers with different output levels. According to the size of gate periphery and number of amplifier cells in the chips, there are two significant differences between the large gate periphery amplifier and the small one. The first one is negative resistance effect and the other is the surface temperature distribution effect.

2.1. Negative Resistance Effect

It can be seen from the high current curves in Fig. 1(a), when the value of voltage between drain to source (V_{ds}) exceeds knee voltage and less than about 20 V, the drain current of the high power amplifier is a little increased with the growth of V_{ds}. Whereas, if the V_{ds} continues to increase, the curve of drain current shows a downward trend. The larger the V_{ds} or the voltage between gate to source (V_{gs}) is, the greater the decreasing margin will be. There are two main reasons for this

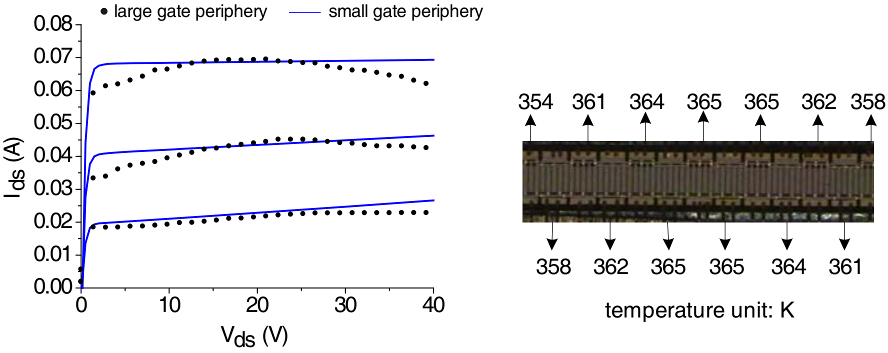

(a) (b)

Figure 1. (a) The current curves of a large gate periphery amplifier and a small gate periphery amplifier. (b) The surface temperature distribution of a large gate periphery amplifier.

phenomenon. The first one is the effect of current collapse. Both surface and buffer donor-like traps can contribute to current collapse through a similar physical mechanism: involving capture of electrons tunneling from the gate and when the device is turned on the trapped electrons is emitted. The effect is very obvious if the electric field under gate electrode is large enough. Although the SiNx passivation weakens the effect, the influence still exists. The second one is the self-heating effect. When the voltages and current are large enough, the channel temperature will increase fast which reduces the mobility and the electron saturation velocity in the channel. As a result, the saturated current will decline.

2.2. Surface Temperature Distributional Effect

Figure 1(b) is the measured temperature result of a high power amplifier chip with large gate periphery, which is collected from the chip surface. The power amplifier contains many amplifier cells with different surface temperatures due to the lager size of the chip. The transverse temperature distribution is determined mainly by the semiconductor materials, metal base, the structure and size of them. Because the heat caused by energy conversion and power combination is mainly concentrated on the center of the chip, the surface temperature of the central amplifier cell will be higher than the marginal one. For the large gate periphery power amplifier, the difference of surface temperature between central amplifier cell and marginal cell is usually more than 20 K. As a result, the output of each amplifier cell is not the same.

The common large signal equivalent circuit models cannot describe the two effects well, so the predicted results cannot be very accurate in the high power and large periphery amplifier. To overcome the problem, an improved I-V large signal equivalent circuit model based on Angelov model is proposed in this research through a series of fitting experiments. The improved empirical equations for large signal equivalent circuit model not only contain the factor of surface temperature, but also embody the negative resistance effect very well.

3. THE DESCRIPTION OF THE IMPROVED I-V MODEL

Fig. 2 shows the AlGaN/GaN HEMT large signal equivalent circuit topology. Typically, there are three main nonlinear elements: source-drain current (I_{ds}), gate-source capacitor (C_{gs}), and gate-drain capacitor (C_{gd}). The variation of the nonlinear equivalent capacitor (such as C_{gs} or C_{gd}) is very small while the variation of I_{ds} is large with the change of the bias voltage or current. So the most significant factor is the I_{ds} in the three nonlinear equivalent elements. The improved I_{ds} model based on the temperature dependence Angelov one is presented as below $[5, 6]$:

$$I_{ds} = I_{pk}(1+\tanh(f_1))(1+f_2V_{ds})\tanh(DV_{ds}) \tag{1}$$

$$f_1 = p_1(V_{gs}-v_{pk})+p_2(V_{gs}-v_{pk})^2+p_3(V_{gs}-v_{pk})^3 \tag{2}$$

$$I_{pk} = \frac{I_{pk0}}{A(V_{ds}^{p}V_{gs}^{q})+BV_{ds}^{0.6V_{gs}}+C}\times\frac{K_t}{\exp(\frac{T-K_2}{K_1})} \tag{3}$$

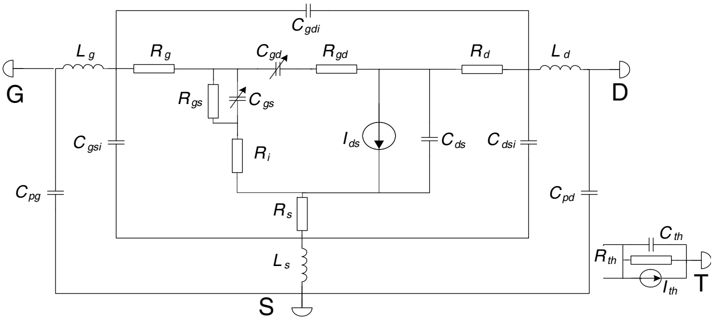

Figure 2. AlGaN/GaN HEMT large signal equivalent circuit topology.

$$v_{pk} = F + GV_{ds} \quad (4)$$

$$f_2 = H \exp\left(M \left|V_{gs}\right|^Q\right) \quad (5)$$

where, V_{ds} is the drain to source voltage, V_{gs} the gate to source voltage, I_{pk} the saturation current, V_{pk} the knee voltage. A, B, C, D, p_1, p_2, and p_3 are constants, and F and G are used to describe the V_{ds} effect on knee voltage caused by short-channel effects. Compared with Angelov model, two main modifications have been added:

(a) Negative resistance effect. The saturation current decreases due to the trapping related dispersion and self-heating effects at high bias voltage, so a compact expression (term including A, B, and C) is added to the denominator of Equation (3) which can embody the phenomenon very well.

(b) Temperature dependent effect. Compared with Angelov model, the exponential function is used instead of linear function in the improved model which is more suitable for the high power amplifier. T represents the surface temperature; K_1, K_2 and K_t are correction factors.

In the improved current model, the location parameter of the amplifier cell is embodied in the surface temperature parameter T. A different T describes a different location of the amplifier cell. There will be as many sets of parameters as there are amplifier cells with different locations. Two methods are presented to identify the surface temperature of each amplifier cell in this research.

3.1. Practical Test

This method needs some accurate testing equipment as Infrared Thermometer. The accurate testing equipment can measure each amplifier cell with the error no more than 1 K which can be neglected in the calculation of I-V formula. Thanks to the large periphery, it is not difficult to distinguish the location of each amplifier cell.

3.2. Simulation Software

Horizontal temperature distribution figure can also be predicted according to the relevant thermodynamics analysis software. Input the structure parameters, material properties, size and other relevant parameters to the software system and then set the central surface temperature of the chip according to the measurement. The horizontal distributional temperature data can be calculated and the figure can be obtained as shown in Fig. 3.

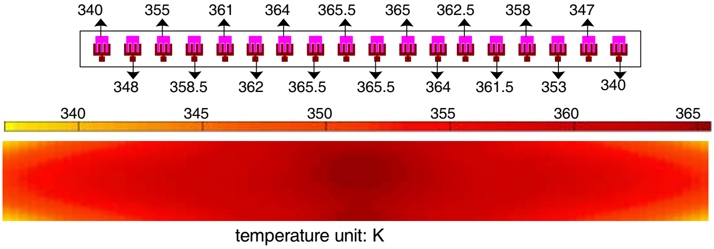

Figure 3. The simulated result of horizontal surface temperature distribution of the amplifier chip.

4. PRACTICAL EXPERIMENTAL VALIDATION

A GaN HEMT power amplifier is measured and modeled to verify the validation and accuracy of the I-V model. The thickness of the silicon carbide (SiC) substrate of the device is 150 μm. The T shape gate is made from Ni/Au with 0.5 μm width. The SiN_x is used as passivation and encapsulation layer. The device consists of a single die (0.85 mm × 5.7 mm chip dimension) with an AuSi eutectic bond to a CMC (Cu/Mo/Cu laminate) ceramic cavity. The power amplifier chip contains 18 cells with the same structure and size. Because of different locations of amplifier cells, each amplifier cell has a different surface temperature T. The outputs of the amplifier cells are combined in the output port. The electroplated gold air-bridge is used as interconnecting approach.

Due to the negative resistance effect and surface temperature, each cell of the high power amplifier is measured and used to validate the proposed model. According to the structure of the power amplifier, there are 18 amplifier cells with different locations and surface temperatures to be measured and modeled using the same I-V formulas. Each amplifier cell has a set of corresponding parameters. As a result, there are a total of 18 sets of parameters constituting a whole current model for the power amplifier. For example, Fig. 4(a) shows the comparisons between the calculated and measured currents of one amplifier cell (marginal cell) under the surface temperature of 330 K, and a good agreement has been achieved with consideration of negative resistance effect. All of the fitting values of the parameters for the marginal amplifier cell in the I-V formulas are shown in Table 1. Fig. 4(b) shows the comparisons of the measured data and calculated I_{ds} of one amplifier cell under different surface temperatures. From the figures, it can be seen that the variations of quiescent bias current under different surface temperatures are obvious which would affect the output of each amplifier cell and total output of the high power

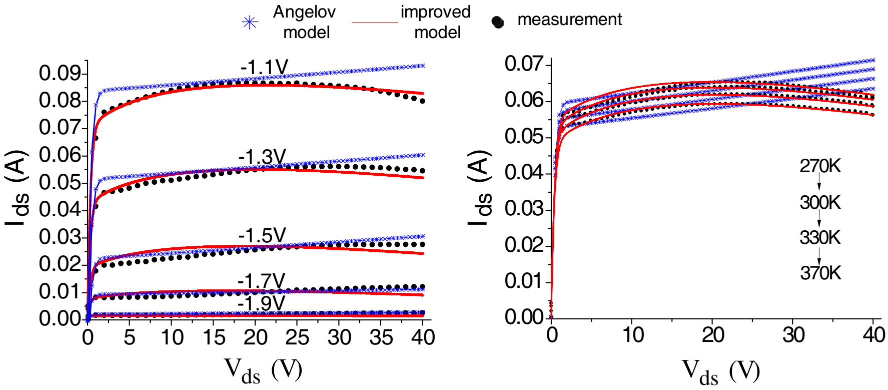

(a) (b)

Figure 4. (a) The predicted I-V curves of one amplifier cell based on Angelov model and improved model compared with measured data. (b) The predicted I-V curves of one amplifier cell compared with measured data under different surface temperatures ($V_{gs} = -1.25\,\text{V}$).

Table 1. The values of parameters for the marginal amplifier cell in the I-V model.

p_1	p_2	p_3	I_{pk0}	A	B	C	D	K_1
−0.594	0.155	0.199	6.653	5.45e-4	−0.0412	1.025	1.909	200

F	G	H	M	Q	p	q	K_t	K_2
1.665	3.33e-3	0.223	−0.096	2.41e-4	0.123	2.746	0.951	300

amplifier.

The linear equivalent elements and parasitic parameters in the equivalent circuit topology of the power amplifier are extracted by using small signal equivalent circuit model (SSECM) based on measured scatter parameters (S-parameter) [7, 8]. The method is described in [7, 8]. The simulated S-parameters compared with the measured data are shown in Fig. 5 with the frequency (f_T) from 0.5 GHz to 4 GHz ($V_{ds} = 28\,\text{V}$, $V_{gs} = -1.3\,\text{V}$). The variation of nonlinear equivalent capacitor (such as C_{gs} or C_{gd}) is very small under the conditions of different bias currents, bias voltages, surface temperatures and levels of output. The Angelov model is accurate enough. So the Angelov nonlinear equivalent capacitors models were used in the research as shown in [6]. All of the models were implemented in Advanced Design System 2009 (ADS) by using

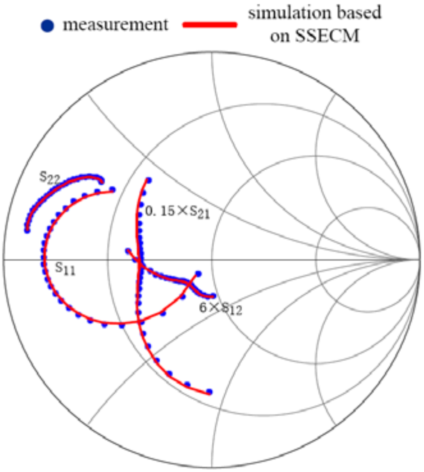

Figure 5. The simulated S-parameters based on SSECM compared with the measurement.

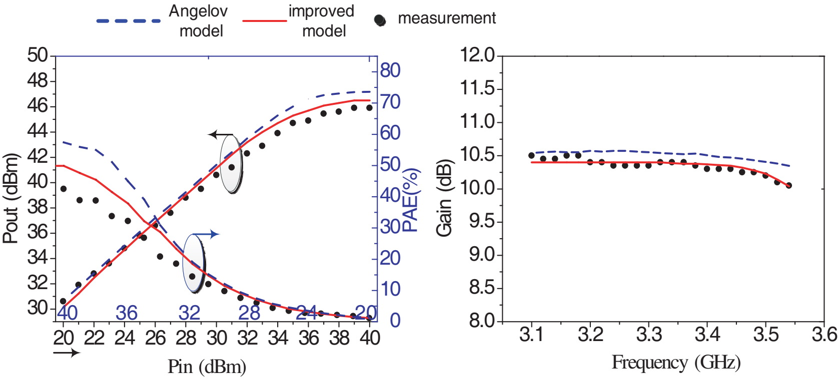

(a) (b)

Figure 6. The simulated results based on the two models compared with measured data. ($f_T = 3.1\,\text{GHz}$). (a) are output and PAE. (b) is Gain versus frequency ($P_{in} = 30\,\text{dBm}$).

symbolic defined devices. The output performances of the device were measured on the load-pull analytic instrument by the conjugate match with the f_T from 3.1 GHz to 3.55 GHz [9–11]. The surface central point was stable at about 365 K by controlling the ambient temperature of the high-low temperature chamber. The V_{ds} was set to 28 V and V_{gs} set to -1.3 V [12–14].

The simulated performance of the high power amplifier based on Angelov model and the improved model are both compared with the measured data. As shown in Fig. 6, when the input and output are small, the predicted data between the two models are very similar. However, when the output of the power amplifier is large enough, the prediction of the improved model is obviously more accurate than the original one. The result can be seen in the comparisons of PAE, output versus input, and Gain versus frequency.

5. CONCLUSION

In order to describe the effect of negative resistance and surface temperature distribution of the high power GaN amplifier with large gate periphery, some improvements need to be added to the I-V equivalent circuit model. In this research, the common temperature dependence Angelov I-V model is used as the original model. The most important advantage of the improved current model is that it can describe the decreasing trend of the current in high voltage which is common in the high output GaN amplifier. The comparisons of the predicted results and measurements show that the improved I-V model can increase the accuracy of large signal equivalent circuit model of the GaN HEMT power device obviously.

ACKNOWLEDGMENT

L. Sang thanks Professor Weng Cho Chew for giving him opportunity to study in the University of Illinois at Urbana-Champaign.

REFERENCES

1. Mishra, U. K., L. Shen, T. E. Kazior, and Y.-F. Wu, “GaN-based RF power devices and amplifiers,” *Proc. of the IEEE*, Vol. 96, No. 2, 287–305, Feb. 2008.
2. Talele, K. and D. S. Patil, “Analysis of wave function, energy and transmission coefficients in GaN/ALGaN superlattice nanostructures,” *Progress In Electromagnetics Research*, Vol. 81, 237–252, 2008.
3. Thein, T. T., C. L. Law, and K. Fu, “Frequency domain dynamic thermal analysis in GaAs Hbt for power amplifier applications,” *Progress In Electromagnetic Research*, Vol. 118, 71–87, 2011.
4. Sang, L., Y. Xu, R. Cao, Y. Chen, Y. Guo, and R. Xu, “Modeling of GaN HEMT by using an improved K-nearest

neighbors algorithm," *Journal of Electromagnetic Waves and Applications*, Vol. 25, No. 7, 2011.

5. Angelov, I., et al., "Extensions of the Chalmers Nonlinear HEMT and MESFET Model," *IEEE Transactions on Microwave Theory And Techniques*, Vol. 44, Oct. 1996.
6. Angelov, I., V. Desmaris, K. Dynefors, P. A. Nilsson, N. Rorsman, and H. Zirath, "On the large-signal modeling of AlGaN/GaN HEMTs and SiC MESFETs," *Gallium Arsenide and Other Semicond. Appl. Symp.*, 309–312, Oct. 2005.
7. Jarndal, A. and C. Kompa, "An accurate small-signal model for AlGaN-GaN HEMT suitable for scalable larger-signal model construction," *IEEE Microwave Wireless Components Letter*, Vol. 16, No. 6, 333–335, Jun. 2006.
8. Lu, J., Y. Wang, L. Ma, and Z. Yu, "A new small-signal modeling and extraction method in AlGaN/GaN HEMTs," *Solid-State Electronics*, Vol. 52, No. 1, 115–120, Jan. 2008.
9. Wong, S.-K., F. Kung, W. Lee, S. Maisurah, and M. N. B. Osman, "A wimedia compliant cmos RF power amplifier for ultra-wideband (UWB) transmitter," *Progress In Electromagnetics Research*, Vol. 112, 329–347, 2011.
10. Lee, M.-W., S.-H. Kam, Y.-S. Lee, and Y.-H. Jeong, "A highly efficient three-stage doherty power amplifier with flat gain for WCDMA applications," *Journal of Electromagnetic Waves and Applications*, Vol. 24, No. 17–18, 2010.
11. Emami, S. D., P. Hajireza, F. Abd-Rahman, H. A. Abdul-Rashid, H. Ahmad, and S. W. Harun, "Wide-band hybrid amplifier operating in S-band region," *Progress In Electromagnetics Research*, Vol. 102, 301–313, 2010.
12. Wu, Y., Y. Liu, S. Li, and S. Li, "A novel high-power amplifier using a generalized coupled-line transformer with inherent DC-block function," *Progress In Electromagnetics Research*, Vol. 119, 171–190, 2011.
13. Choi, H., Y. Jeong, C. D. Kim, and J. S. Kenney, "Bandwidth enhancement of an analog feedback amplifier by employing a negative group delay circuit," *Progress In Electromagnetics Research*, Vol. 105, 253–272, 2010.
14. Zhang, B., Y.-Z. Xiong, L. Wang, S. Hu, T.-G. Lim, Y.-Q. Zhuang, and J. L.-W. Li, "A D-band power amplifier with 30-GHz bandwidth and 4.5-dBm psat for high-speed communication system," *Progress In Electromagnetics Research*, Vol. 107, 161–178, 2010.